Applied Physics A (2021) 127:41
https://doi.org/10.1007/s00339-020-04202-0

Applied Physics A
Materials Science & Processing

Effect of Mn codopant on thermoluminescence properties of γ-rays irradiated $Na_3Y(PO_4)_2$:Dy phosphors for dosimetry applications

K. Munirathnam[1] · P. C. Nagajyothi[2] · K. Hareesh[1] · M. Madesh Kumar[1] · S. D. Dhole[3]

Received: 5 October 2020 / Accepted: 8 December 2020 / Published online: 3 January 2021

Abstract

Orthophosphate-based phosphors have been used widely as efficient materials for the luminescence applications. Thermoluminescence (TL) properties of luminescent materials help us to find the suitability of the phosphors for the TL dosimetric application. In this work, a series of Dy^{3+} doped and Mn^{2+}-codoped sodium yttrium phosphate $Na_3Y(PO_4)_2$ phosphors were synthesized via a solid-state reaction method and thermoluminescence behavior were studied. To observe the effect of the dopant and codopants on phase purity and crystalline structure of phosphors, X-ray diffraction method analyses were carried. In addition, the morphological images were examined; chemical composition and functional groups were confirmed. Herein, the Dy^{3+}-doped and Mn^{2+}-codoped $Na_3Y(PO_4)_2$ phosphors were irradiated by 1 kGy-dose γ-radiation and $Na_3Y(PO_4)_2$:0.07Dy^{3+} showed a intense TL intensity peak at 178 °C, whereas Mn^{2+}-$Na_3Y(PO_4)_2$:0.07Dy^{3+}, 0.07Mn^{2+} phosphors showed at 134 °C. The effect of codopant Mn^{2+} on the TL properties of Dy^{3+}-doped $Na_3Y(PO_4)_2$ phosphors and irradiation dose were investigated. The optimized $Na_3Y(PO_4)_2$:0.07Dy^{3+} phosphor was showed a linear response to irradiation as a function of dose in the range of the 50 Gy–1.5 kGy. The glow curves were deconvolated and the TL kinetic parameters of phosphors were obtained by adopting various methods, revealing that the glow curves exhibited the second-order kinetics, and activation energies were calculated. The kinetic parameters of prepared samples were compared with the other TL materials. The obtained results confirm that the phosphors may have potential applications as TL dosimetry materials to measure low irradiation.

Keywords Phosphors · Thermoluminescence · Dosimetry

1 Introduction

Thermoluminescence (TL) is a versatile technique owing to its wide spread application in diverse fields such as dosimetry of high- or low-energy radiation, radiation therapy, agriculture/food irradiation sciences, and space research [1, 2]. In TL dosimetry (TLD), phosphors play a vital role because of their excellent TL properties such as high efficiency, radiation dose response, thermal stability, high sensitivity, and reproducibility [3, 4]. Generally, the TL emission occurs when electron and hole traps, that are formed due to irradiation by high-energy radiation in dosimetry materials, which are stimulated by thermal energy and recombined [5]. The TL emission is directly proportional to the irradiation dose that is absorbed by phosphor materials, and therefore, the unknown radiation can be measured. The phosphors are prepared by doping rare-earth ions or transition ions that create traps in the TL material by introducing luminescence centers rather than damage to their crystal structure. Specifically,

Supplementary Information The online version contains supplementary material available at https://doi.org/10.1007/s00339-020-04202-0.

✉ K. Munirathnam
mail2rathnam@gmail.com

✉ P. C. Nagajyothi
pcnnagajyothi@gmail.com

[1] Department of Physics, School of Applied Sciences, REVA University, Bangalore, India

[2] School of Mechanical Engineering, Yeungnam University, Gyeongsan 38541, South Korea

[3] Department of Physics, Savitribai Phule Pune University, Pune 411007, India

luminescence of Dy^{3+} ions produce excellent luminescence emission in the visible part of the electromagnetic spectrum and emission from these ions strongly depends on site symmetry of the host matrix around the ions [6]. The Dy^{3+} ion-doped $CaSO_4$ (TLD-900) is always the preferred choice commercially to measure lower dose range in the fields of nuclear medicine, radiology, and radiation research using smaller radioactivity. Additionally, the transition metal ions Mn^{2+} can also produce a broad band emission in the visible range from green to red depending on the around crystal field owing to its d–d transition. The Mn ion-activated $CaSO_4$ has been reported as a sensitive material and it gives TL intense glow peak at a low-temperature regions. Moreover, the emission spectrum of Dy^{3+} ions matches with the excitation spectrum of Mn^{2+} ions, and therefore, Mn^{2+} ions have been used as the sensitizer for luminescence [5, 7, 8]. There are several commercially available rare-earth- and transition-ion-doped TLD phosphors. For an instance, CaF_2:Dy(TLD-200), CaF_2:Mn(TLD-400), $CaSO_4$:Dy, Mn, and $Li_2B_4O_7$:Mn (TLD-800) phosphors are commercially available [5, 7–9]. However, every phosphor has its own drawbacks such as toxicity, low reusability, reliability, lack of tissue equivalence, and sensitivity; therefore, it is necessary to synthesis the novel material for reliable dosimeters in the radiation-related fields [10].

Generally, phosphate-based phosphors have excellent TL properties and are used as optically stimulated luminescence materials because of their chemical and thermal stabilities, resistance to radiation damage, non-hygroscopic nature, high absorption coefficient, and high luminescence output [11–14]. The TL properties of some phosphate-based materials were reported by researchers, namely, $Sr_2P_2O_7$:Eu^{3+} [15], $NaLi_2PO_4$:Eu^{3+} [2], $LuPO_4$:Eu [13], $NaCaPO_4$:Dy^{3+} [16], and $Li_2BaP_2O_7$:Dy^{3+} [17]. Furthermore, the TL properties of phosphate-based materials can be enhanced further by γ-irradiation. Gamma radiation creates energy traps between the valence and conduction bands, which decreases the recombination rate of electron–hole pairs, thereby increasing the TL properties of phosphate materials. In this context, Batal et al. [18] studied the absorption spectra of gamma-irradiated sodium phosphate glasses containing vanadium, and observed the formation of characteristic defects and color centers, the possible photochemical effect of the transition metal in the glass, and the possible approach of saturation after a certain irradiation dose. Tsai et al. [19] investigated the effect of gamma radiation on the structure and properties of single-phase tetracalcium phosphate, which showed a lower porosity volume fraction or compressive strength at low gamma doses (10 and 20 kGy) and more porous/loose and apatite particles became larger in size at high gamma doses (after 30 kGy). Gamma radiation-induced defect centers in undoped phosphate glasses and the effect of these centers on the sensitivity and build-up time of silver-doped phosphate glasses were investigated by Fan et al. [20]. The thermoluminescence of beta-irradiated $Ca_5(PO_4)_3OH$:Gd^{3+},Pr^{3+} was reported and activation energy as well as the frequency factor for different TL curve peaks determined by Mokoena et al. [21]. The optical properties, such as photoluminescence and radio-photoluminescence (RPL) of various X-ray irradiated Ag-doped phosphate glasses, were investigated by Tanaka et al. [22]. Recently, Kodaira et al. [23] used Ag^+-activated phosphate glass as an RPL dosimeter for heavy ions (from C to Fe) and estimated a linear energy transfer (LET) threshold of 5 keV/μm in water. They also argued that the Ag^+-activated phosphate glass had good potential for application in fluorescent nuclear track detectors for high LET range (5–200 keV/μm) radio-immunotherapy and space radiation dosimetry.

From the literature reviews, it can be conclude that γ-irradiated phosphate-based phosphor doped with rare earths and transition ions have been widely used for radiation dosimetry application. However, there are no reports on the Dy-doped and Mn-codoped sodium yttrium phosphate $Na_3Y(PO_4)_2$ phosphors as a TL dosimeter. The selected double sodium rare-earth phosphates host material $Na_3Y(PO_4)_2$ has the fundamental building blocks of the separated PO_4 tetrahedral and Na^+ and RE^{3+} ions lying among them, which shares oxygen ions to form the rare-earth REO_6 octahedral; these are suitable for accommodating rare-earth ions and transition ions in the host and may create traps on excitation [24]. Therefore, in this present work, $Na_3Y(PO_4)_2$ has been doped with Dy^{3+} and codoped with Mn^{2+} was irradiated by gamma radiation and TL properties were studied. The results showed good linear response with respect to gamma dose, suggesting its potential application as a gamma dosimeter.

2 Synthesis

2.1 Preparation of phosphors

A series of Dy^{3+}-doped $Na_3Y(PO_4)_2$ and $Na_3Y(PO_4)_2$:$0.07Dy^{3+}$, yMn^{2+}phosphors were prepared by the high-temperature solid-state reaction (SSR) method. Initially, Na_2CO_3, Y_2O_3, $NH_4H_2PO_4$, Dy_2O_3, and $MnCO_3$ were taken as starting materials (all were of analytical reagent grade) and weighed in stoichiometric amounts according to the balanced chemical equations for synthesis as follows.

1. For Dy^{3+}-doped $Na_3Y(PO_4)_2$:

$$3Na_2CO_3 + xDy_2O_3 + (1-x)Y_2O_3 + 8NH_4H_2PO_4 \rightarrow 2Na_3Dy_xY_{(1-x)}(PO_4)_2 + 3CO_2 + 8NH_3 + 6H_2O.$$

2. For Dy^{3+}-doped and Mn^{2+}-codoped $Na_3Y(PO_4)_2$:

$$(3-y)Na_2CO_3 + xDy_2O_3 + yMnCO_3 (1-x)Y_2O_3 + 8NH_4H_2PO_4 \rightarrow 2Na_{(3-y)}DyY_{(1-x)}(PO_4)_2 + 3CO_2 + 8NH_3 + 6H_2O.$$

To eliminate NH_4, CO_2, and water from the homogeneity mixtures, the samples were heated slowly to 400 °C, maintained at 900 °C (10 h), and finally heated at 1100 °C for 5 h in ambient air with several intermediate grindings and subsequently cooled to room temperature (23 °C) in the furnace. Furthermore, the sintered materials were ground into fine powders and subjected to irradiation and characterization.

2.2 Gamma irradiation of phosphate materials

The as-prepared phosphate materials were exposed to a Co-60 gamma source at different doses ranging from 50 Gy to 1.5 kGy with dose rate of 5.4 kGy/h. The radionuclide Co-60 ($^{60}Co_{27}$) is most commonly used source of gamma radiation with half-life 5.27 years. Co-60 radioactive source can be produced by exposing Co-59 to neutrons in nuclear reactor. Co-60 decays into a Ni-60 ($^{60}Ni_{28}$) principally emitting one negative beta particle (maximum energy is 0.318 MeV). Thus, produced Ni-60 is in excited state, and it immediately emits two photons of energy 1.173 MeV and 1.333 MeV in succession to reach its stable state. These two gamma rays are responsible for radiation processing in the Co-60 gamma irradiators. Therefore, the average energy of gamma rays is considered as 1.25 MeV [25]. The schematic representation of decay scheme of Co-60 is shown in Fig. 1.

2.3 Characterization

Pristine and gamma radiation-irradiated phosphate materials were characterized. The powder X-ray diffraction (XRD) patterns were recorded using a diffractometer (PANalytical X'Pert PRO, USA) with Cu K_α radiation of wavelength λ =1.5405 Å, and 2θ was recorded in the range of 10–60°. The IR spectra were recorded by Fourier transform infrared (FTIR) spectroscopy in the range of 4000–400 cm^{-1} on an IR spectrometer (Perkine Elmer, Bruker). Scanning electron microscopy (SEM; ZEISS EVO MA 15) was employed to examine the distribution of the synthesized particles, and surface morphological graphs were captured. The elemental composition of the phosphor powders was evaluated using energy-dispersive spectroscopy (EDS) equipped with an X-ray detector (THERMO EDS) coupled with the SEM instrument. For the thermoluminescence measurements, all the $Na_3Y(PO_4)_2$:xDy^{3+} (x = 0.03,0.05,0.07, and 0.09) samples were irradiated with 1 kGy gamma radiation for 30 min. The Dy^{3+} concentration was fixed at x = 0.07, and the Mn^{2+} concentration was varied (y = 0.01, 0.03, 0.05, 0.07, and 0.09) to study the effect of irradiation on the samples. Furthermore, $Na_3Y(PO_4)_2$:$0.07Dy^{3+}$ was irradiated with various radiation dose from 50 Gy to 1.5 kGy. The TL glow curves were measured using an NUCLEONIX TL analyzer type TL1009 TL reader at a heating rate of 2.5 s^{-1} in the temperature range from 303 to 673 K.

3 Results and discussion

3.1 Structural and morphological studies

Figure 2 shows the typical XRD patterns of $Na_3Y(PO_4)_2$:xDy^{3+}, yMn^{2+}. All the diffraction peaks were well matched with the XRD profile of the monoclinic $Na_3Y(PO_4)_2$ phase obtained in solid state at 1100 °C, as reported by Matraszek et al. [26]. The results showed that the synthesized samples exhibited a single phase and no significant phase changes occurred even after doping and codoping the host matrix with Dy^{3+} and Mn^{2+} ions, respectively. Possibly, the Dy^{3+} ions with radii of 0.103 nm (CN = 8) were situated in the Y^{3+} ion sites with radii of 0.102 nm (CN = 6),

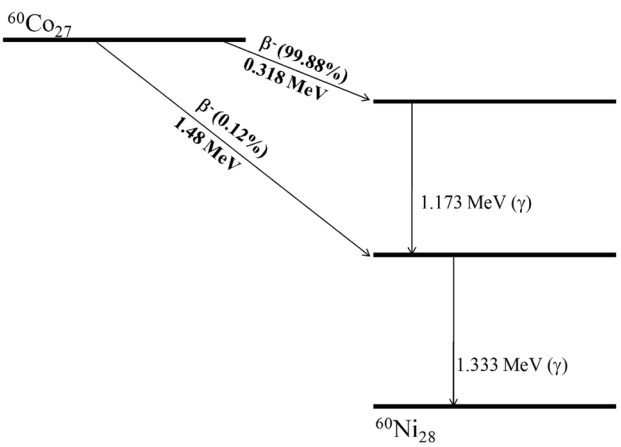

Fig. 1 Schematic representation of Co-60 gamma source

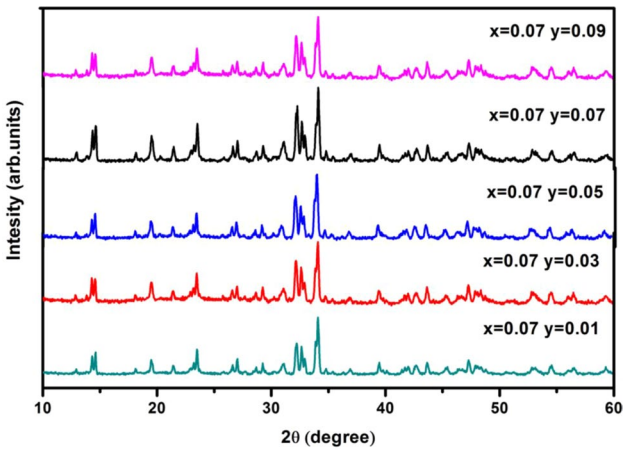

Fig. 2 Typical XRD profile of $Na_3Y(PO_4)_2$:xDy^{3+}, yMn^{2+}

where the radii of the dopant ions were nearly equal to that of the host ions and the charges were balanced as shown in the below equation:

$$Dy^{3+} \rightarrow Y^{3+} + Dy_Y^0. \quad (1)$$

Similarly, Mn^{2+} ions with radii of 0.96 nm (CN = 8) could be situated in the Na^+ ion sites with radii of 0.118 nm (CN = 8), where the radii of the ions were equal and thus, the charges could be balanced as:

$$Mn^{2+} \rightarrow 2Na^+ + Mn_{Na}^0 + V''_{Na}. \quad (2)$$

Here, by creating oxygen vacancies in the host materials. Therefore, the incorporation of dopant Dy^{3+} ions at sites of Y^{3+} and codopant Mn^{2+} ions at sites of Na^+ is more likely to occur in the host matrix [27].

Figure 3 shows the FTIR spectra of $Na_3Y(PO_4)_2$:xDy^{3+},yMn^{2+} phosphors. The strong and broad IR absorption peaks in the range of 490–400 cm^{-1} and 650–520 cm^{-1} were attributed to the asymmetric and symmetric deformation modes of the phosphate group (PO_4), respectively. The weak absorption peaks in the range of 950–840 cm^{-1} arose due to symmetric stretching (PO_4), and the broad peak at 1130–990 cm^{-1} was attributed to the asymmetric stretching of PO_4 groups. The IR absorption peaks confirmed that the prepared phosphors had PO_4 groups. Moreover, no absorption peaks were found in the range of 3654–3535 cm^{-1}, revealing that the prepared samples were free from moisture and nonbonding phosphor with hydroxyl groups [28, 29].

The SEM image and energy-dispersive X-ray (EDX) spectrum of $Na_3Y(PO_4)_2$:$0.07Dy^{3+}$,$0.03Mn^{2+}$ are presented in Fig. 4a, b, respectively. The morphological analysis showed that the particles had equal sizes in the range of 3–5 µm, and the EDX spectrum revealed the presence of Na, Y, P, and O in the compound. Moreover, there was no evidence of the presence of impurities in the host matrix, which supported the XRD results.

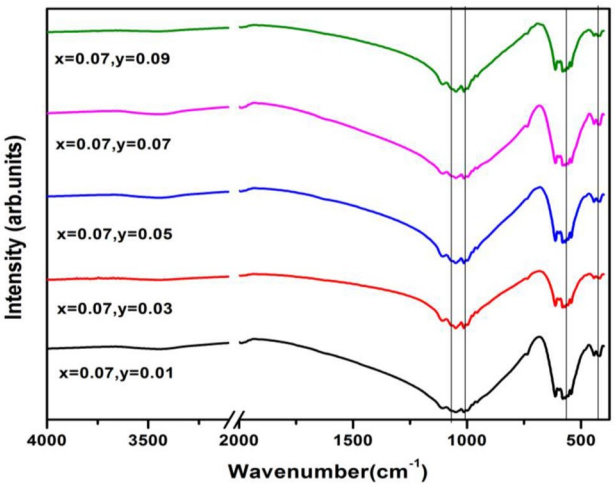

Fig. 3 Typical FTIR spectra of $Na_3Y(PO_4)_2$:xDy^{3+}, yMn^{2+}

3.2 TL studies

3.2.1 Evaluation of trap parameters from glow curve deconvolution

TL properties can be studied from the kinetic parameters obtained from the TL glow curve, which represents the intensity of the emitted light as a function of temperature. It is well known that the kinetic parameters provide information regarding the suitability of phosphors for dosimetric applications, the mechanism of state/charge traps in the material, and the formation of localized energy levels within the forbidden gap for TL emission in the material [30]. In general, the TL emission of phosphors is highly dependent on the type of traps/luminescent centers created by irradiation, dopant concentration, and annealing temperature.

Herein, the TL material $Na_3Y_{1-x}(PO_4)_2$:xDy^{3+}, yMn^{2+} was prepared by doping with Dy^{3+} ions (x = 0.01,0.03,0.05,0.07, and 0.09), and codoping with yMn^{2+} ions (y = 0.01,0.03,0.05,0.07, and 0.09), where Dy^{3+} ion (x = 0.07) concentration was kept constant. The prepared phosphors were subjected to gamma ray doses of 1 kGy prior to TL measurements, and the TL glow curves were recorded and are presented in Fig. 5. From TL curve, it was observed that $Na_3Y_{1-x}(PO_4)_2$:$0.3Dy^{3+}$ phosphor was found to have two strong peaks at low temperature (103 °C) and at high temperature (205 °C), and one weak peak at 300 °C, potentially because the sample possesses increased numbers of shallow traps at low temperatures as well as at high temperature. On the increasing dopant concentration, three peaks were slowly disappeared and found to have single peak, the possible reason may be decrease in trap levels in the host materials due to dopant concentration. However, the TL emission increased with dopant concentration up to $0.7Dy^{3+}$ ions and subsequently decreased at higher concentrations. The $Na_3Y_{1-x}(PO_4)_2$:xDy^{3+} (x = 0.07, 0.09) phosphors showed abroad TL emission peak with an appropriate Gaussian shape at 178 °C, which is suitable for TL application [31]. To study the TL behavior of phosphors, kinetic parameters such as the order of kinetics (β), activation energy/trap depth (E), and frequency factor(s) can be obtained by employing various methodology based on the shape or geometrical properties of TL glow peaks. Herein, three methods such as Chen's, Lushihik, and Halperin–Braner methods were followed to analyze the deconvoluted TL

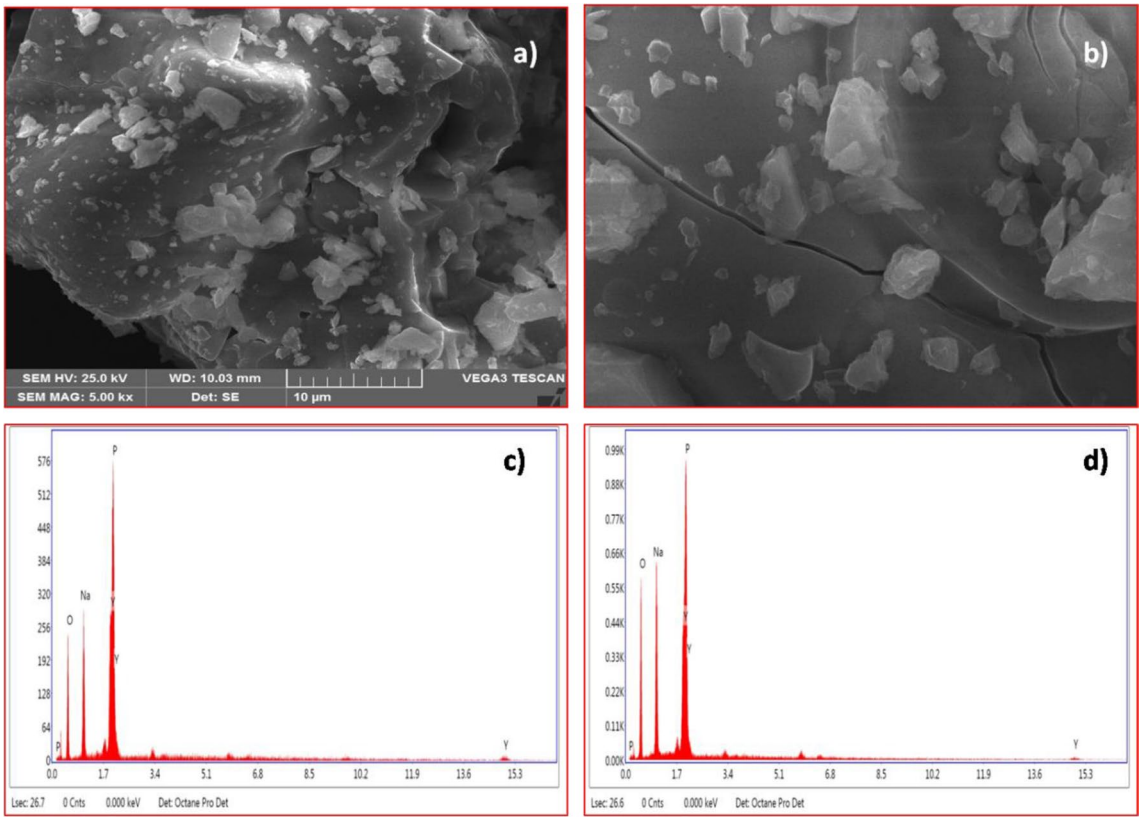

Fig. 4 Typical **a** SEM image of $Na_3Y(PO_4)_2$:0.07Dy^{3+}, 0.03Mn^{2+}; **b** $Na_3Y(PO_4)_2$:0.07Dy^{3+}, 0.09Mn^{2+}; **c** and **d** corresponding EDX spectrum, respectively

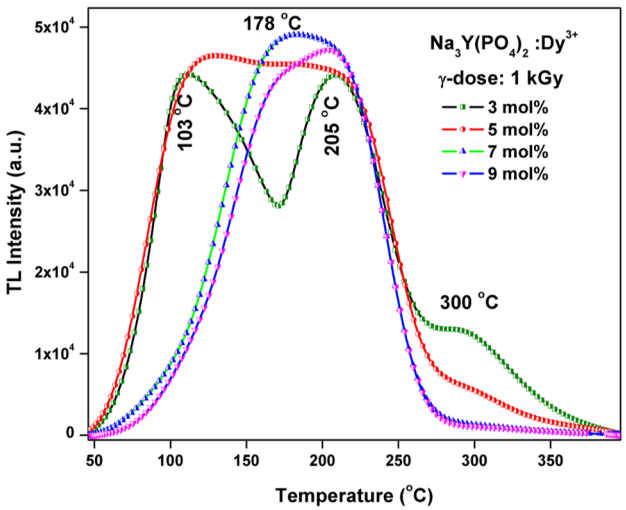

Fig. 5 TL glow curves of $Na_3Y_{1-x}(PO_4)_2$:xDy^{3+}

glow curves that suite best for obtained peaks from the TL measurements. At first, the equations derived from Chen's approach were adopted, which solves various difficulties include no complicated iterative methods. The Chen's new approximation equation for second-order kinetics to determine the activation energy ($E\gamma$) is given as follows [32]:

$$E_C = 2kT_m\left(\frac{1.756T_m}{\omega} - 1\right), \tag{3}$$

where T_m = temperature at the maximum peak and $\omega = T_2 - T_1$(T_1, T_2 are the temperatures on either side of T_m). The kinetic order was calculated using the following equation $\mu_g = \delta/\omega$ (where $\delta = T_2 - T_m$). The frequency factor(s) was evaluated using the Chen–Winner equation [33]:

$$s = \frac{\beta E}{kT_m^2}\exp\left(\frac{E}{kT_m}\right)\left[1 + (b-1)\Delta_m\right]^{-1}, \tag{4}$$

where E is the activation energy, b is order of kinetics, $\beta = 2.5$ °C/s is heating rate and $\Delta_m = \frac{2kT_m}{E}$.

The total number of trapped electrons (n_o) can be calculated by adopting the general-order kinetics model to fit the TL curve [33]:

$$I(T) = \frac{s}{\beta}n_0\exp\left(-\frac{E}{kT}\right)\left[1 + \frac{(b-1)s}{\beta}\int_{T_0}^{T}\exp\left(-E/kT'\right)dT'\right]^{-b(b-1)}, \tag{5}$$

where s is the frequency factor that is considered as a constant, E is the activation energy/trap depth, and b is the kinetic order. The experimental data were obtained from the TL glow curves.

Furthermore, to verify the activation energy, here, two more methods were adopted, the one is proposed by Lushihik and the other one suggested by Halperin–Braner for second-order kinetics. The evaluation of the activation energy for second-order kinetics was performed using Lushihik's formula as given by [34]:

$$E_L = 1.706\left(\frac{kT_m^2}{\delta}\right), \tag{6}$$

where $\delta = T_2 - T_m$.

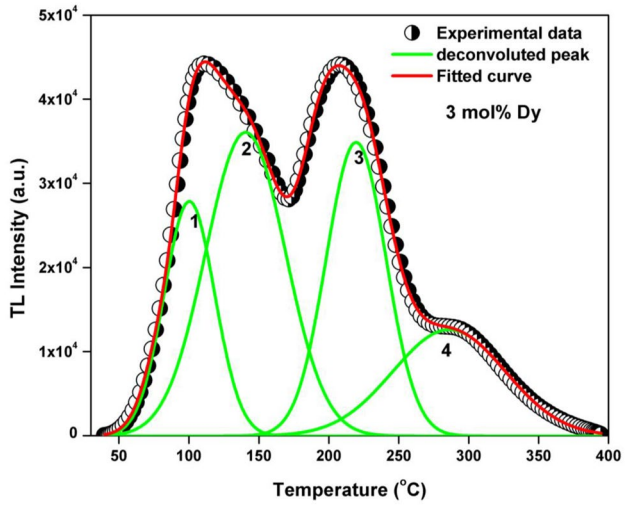

Fig. 6 Deconvoluted TL glow curve of $Na_3Y_{1-x}(PO_4)_2$:0.03Dy^{3+}

The another approach suggested by Halperin–Braner uses an iterative process to find E using both T_1 and T_2 on the glow curve [35], as demonstrated by the following equation:

$$E_{HB} = \frac{2kT_m^2}{\tau}(1 - 3\Delta_m) \tag{7}$$

where, $\Delta_m = \frac{2kT_m}{E}$ and $\tau = T_m - T_1$.

For further analysis, all TL graphs of the prepared phosphors were deconvoluted, and the typical $Na_3Y_{1-x}(PO_4)_2$:xDy^{3+} ($x = 0.03$) curve is shown in Fig. 6. The calculated values of activation energy using different methods along with the values of other parameters are summarized in Table 1.

The activation energies of $Na_3Y_{1-x}(PO_4)_2$:xDy^{3+}($x = 0.03$) were calculated by all three methods for the peak at low temperature (103 °C) found to be nearly 2.825 eV, whereas for other dopant concentration, it is was very less, which reveals the less number of trapping levels at higher concentration. The activation energies for different deconvolation peaks were different, which information about the formation of some shallow and some deep traps. The kinetic order (μ_g) was calculated for all the peaks, and the shape factors for all the peaks and samples were in the range of 0.47 to 0.50, which conformed that the phosphor showed the second-order kinetics.

3.2.2 Linear dose response

To study the linear response of phosphors to the radiation dose, $Na_3Y_{1-x}(PO_4)_2$:xDy^{3+}($x = 0.07$) was irradiated with various doses of γ-radiation. The TL glow curves with TL intensity as a function of accumulated radiation dose were recorded and are shown in Fig. 7. The TL intensity signal increased linearly with γ-radiation (regression

Table 1 TL trap parameters of $Na_3Y_{1-x}(PO_4)_2$:xDy^{3+}($x = 0.03$,0.05,0.07, and 0.09)

Dopant Dy^{3+} %	Peaks	T_m (K)	μ_g(b)	Activation energy (eV)			Frequency factor (s-1)	Electron concentration (n_o)
				Chen	Lushchik	Halperin and Braner		
3	1	110	0.50 (2)	2.825	2.918	2.792	1.08E+17	2E+05
	2	145	0.48 (2)	0.588	0.521	0.577	1.373E+08	5.00E+06
	3	298	0.50 (2)	0.682	0.676	0.651	6.443E+07	6.00E+06
5	1	100	0.48 (2)	1.02	1.079	1.007	4.85E+17	3E+05
	2	148	0.48 (2)	0.443	0.486	0.448	3.199E+08	4.00E+06
	3	209	0.50 (2)	0.319	0.355	0.314	1.085E+05	9.00E+06
7	1	118	0. 48 (2)	0.642	0.665	0.617	6.04E+10	3.00E+06
	2	156	0.50 (2)	0.601	0.604	0.606	2.18E+09	5.00E+06
	3	308	0.48 (2)	0.639	0.66	0.628	9.797E+06	6.00E+06
9	1	121	0.48 (2)	0.315	0.389	0.395	8.31E+16	4.00E+06
	2	152	0.50 (2)	0.583	0.554	0.558	2.81E+10	5.00E+06
	3	268	0.51 (2)	0.439	0.464	0.406	6.411E+05	1.00E+07

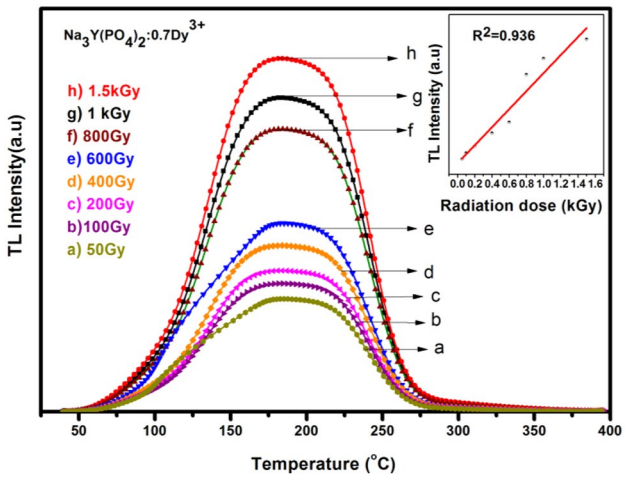

Fig. 7 Linear response TL glow curve of $Na_3Y_{1-x}(PO_4)_2$:0.07Dy^{3+}

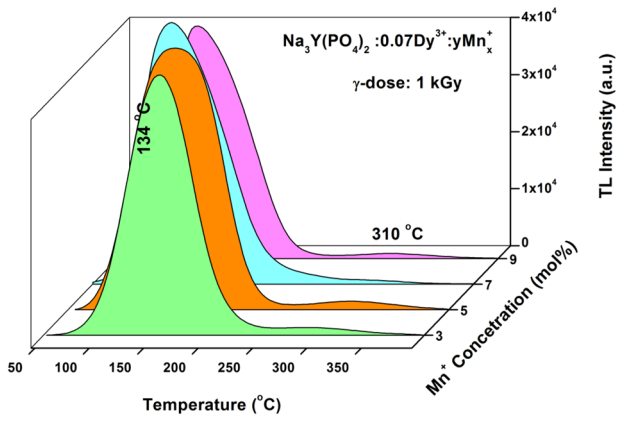

Fig. 8 TL glow curve of $Na_3Y_{1-x}(PO_4)_2$:0.07Dy^{3+}, $y$$Mn^{2+}$($y$ = 0.03,0.05,0.07, and 0.09)

coefficient = 0.936) and was proportional to the gamma dose from 50 Gy to 1.5 kGy (shown in the inset). The TL curves were found to have a broad single peak at 178 °C, which was maintained for the different radiation doses. Moreover, no TL saturation was found under 1.5 kGy, which may be because the radiation dose does not affect electron–hole pair trap recombination. The high radiation dose may lead to reduction in the space between electron and hole pair traps or the distance between luminescence centers and the limited number of available vacant traps in the TL material [36]. Another reason for the high-dose response might be the effective atomic number (Z_{eff}) of the TL material. It is well known that phosphor materials have a high Z_{eff} that usually responds to relatively high-dose ranges, which can be more useful for high-dose radiation applications. The Z_{eff} of $Na_3Y(PO_4)_2$:Dy^{3+} is approximately 48, which may be expected to show a TL response to high radiation doses [31]. Hence, the linear response of the prepared phosphors to irradiation and high-dose response is an important characteristic for application in TL dosimetry.

3.2.3 Effect of Mn^{2+} codopant on TL properties

To study the effect of the codopant on the TL properties, the concentration of dopant Dy^{3+} ions was kept constant at $Na_3Y_{1-x}(PO_4)_2$:xDy^{3+} (x = 0.07) (which showed the maximum TL intensity), and the Mn^{2+} ion concentration was varied and exposed to 1 kGy radiation. The recorded TL glow curves are shown in Fig. 8. The TL intensity increased with codopant concentration up to y = 0.07 and then decreased. The glow curves consisted of two peaks a broad peak at 134 °C and a weak peak at 310 °C, whereas the $Na_3Y_{1-x}(PO_4)_2$:xDy^{3+} (x = 0.07) phosphor exhibited only one TL signal peak at 178 °C. The maximum peak temperature decreased due to codoping with Mn^{2+} ions in the host material and the TL intensity also decreased; the possible reason behind this decrease may be the limited electron–hole charge traps or decreased distance between luminescence centers. The weak peak at 310 °C is purely due to Mn^{2+} ions forming luminescence centers [37]. The calculated trap parameters are tabulated in Table 2, and various phosphate-based TL materials are compared and shown in Table 3. From the comparison, it can be concluded that the Dy^{3+}-doped and Mn^{2+}-codoped $Na_{3-y}Y_{1-x}(PO_4)_2$ phosphor may be a potential TL material for TLD applications.

4 Conclusion

In summary, Mn^{2+}-codoped $Na_3Y_{1-x}(PO_4)_2$:0.07Dy^{3+} phosphors were prepared by an solid-state reaction for TL gamma radiation dosimetry. The TL glow curves of all Dy^{3+}-doped $Na_3Y(PO_4)_2$ were in the appropriate Gaussian shape with a peak at 178 °C and $Na_3Y_{1-x}(PO_4)_2$:0.07Dy^{3+} exhibited the maximum TL intensity, whereas $Na_3Y_{1-x}(PO_4)_2$:0.03Dy^{3+} showed the three peaks at 103 °C, 205 °C, and 300 °C, and it can be used to measure radiation in the low as well as high-temperature regions. The Mn^{2+} ions codoped with $Na_3Y_{1-x}(PO_4)_2$:0.07Dy^{3+} phosphors had two peaks at 134 °C and 310 °C. The kinetic parameters of activation energy, the order of kinetics, and frequency factors were established by Chen's new approximation method and found that the values of activation energy ranged from 2.91 to 0.46 eV . The TL curves were belongs to second order of kinetics, frequency factor(s) Furthermore, Lushihik, Halperin, and Braner method were adapted to analyse activation energy and obtained values were consisting with Chen's new approximation method. The trap parameters and linear response suggested that the prepared phosphors may be good potential candidates for TLD applications.

Table 2 TL trap parameters of $Na_3Y_{1-x}(PO_4)_2$:0.07Dy^{3+}, yMn^{2+}(y = 0.03,0.05,0.07, and 0.09)

Mn^{2+}%	Peaks	T_m (K)	$\mu_g(b)$	Activation energy (eV)			Frequency factor (s-1)	Electron concentration (n_o)
				Chen	Lushchik	Halperin and Braner		
3	1	134	0.47 (2)	0.567	0.511	0.562	2.4 E + 10	4.00E + 06
5	1	134	0.49 (2)	0.433	0.476	0.426	1.2 E + 08	3.00E + 06
	2	310	0.48 (2)	0.329	0.345	0.308	1.085E + 07	5.00E + 06
7	1	134	0.50 (2)	0.611	0.594	0.610	2.18E + 09	4.00E + 06
9	1	134	0.49 (2)	0.573	0.534	0.498	1.91E + 10	4.00E + 06
	2	310	0.50 (2)	0.429	0.434	0.396	5.411 E + 07	1.00E + 07

Table 3 Comparison of various phosphate-based TL materials with prepared samples

TL material	γ-Radiation dose	TL intensity (a.u)	E (eV)	S^{-1}	Coefficient of linearity
$Na_3Y(PO_4)_2$: Dy^{3+}	1 kGy	5×10^4	2.825	1.08×10^{17}	0.936
$Na_3Y(PO_4)_2$:0.07Dy^{3+}, 0.03Mn^{2+}	1 kGy	4×10^4	0.567	4.00×10^{06}	–
$Li_2BaP_2O_7$:Dy [17]	45 Gy	1.6×10^6	1.81	1.41×10^{13}	0.9956
$CaSO_4$:Dy [5, 17, 38]	45 Gy	5×10^8	1.145	6.78×10^{12}	0.9958
CaSO4:Dy, Mn [5]	1 Gy	5×10^5	0.841	5.5×10^7	0.9995

The thermoluminescence study on the codoped phosphor suggests its stability to low dose of γ-ray exposure.

Acknowledgements One of the authors, Dr. K. Munirathnam, is deeply thankful to The Honorable Dr. P. Shyama Raju, Chancellor of REVA University, Bangalore, INDIA, for providing financial assistance to carry out this research work. This work was supported by the National Research Foundation of Korea funded by the Korean government (MSIP-2018R1A2B6006056).

Compliance with ethical standards

Conflict of interest The authors declared that there is no conflict of interest.

References

1. B.P. Kore, N.S. Dhoble, K. Park, S.J. Dhoble, Photoluminescence and thermoluminescence properties of Dy^{3+}/Eu^{2+} activated $Na_{21}Mg(SO_4)_{10}Cl_3$ phosphors. J. Lumin. **143**, 337–342 (2013)
2. M. Singh, P.D. Sahare, P. Kumar, Synthesis and dosimetry characteristics of a new high sensitivity TLD phosphor $NaLi_2PO_4$:Eu^{3+}. Radiat. Meas. **59**, 8–14 (2013)
3. M.T. Jose, S.R. Anishia, O. Annalakshmi, V. Ramasamy, Determination of hermoluminescence kinetic parameters of thulium doped lithium calcium borate. Radiat. Meas. **46**, 1026–1032 (2011)
4. M. Klosowski, L. Czopyk, K. Kisielewicz, D. Kabat, P. Olko, M.P.R. Waligorski, Novel thermoluminescence foils for 2-D clinical dosimetry, based on $CaSO_4$:Dy. Radiat. Meas. **45**, 719–726 (2010)
5. S. Bahl, S.P. Lochab, P. Kumar, $CaSO_4$:Dy, Mn: a new and highly sensitive thermoluminescence phosphor for versatile dosimetry. Radiat. Phys. Chem. **119**, 136–141 (2016)
6. A.R. Kadam, G.C. Mishra, S.J. Dhoble, Thermoluminescence study and evaluation of trapping parameters CaTiO3: RE (RE = Eu3+, Dy3+) phosphor for TLD applications. J. Mol. Struct. **1225**, 129129–129138 (2020)
7. Su. Qiang, C. Li, H. He, Lu. Yuhua, J. Li, Ye. Tao, Luminescent materials and spectroscopic properties of Dy^{3+} ion. J. Lumin. **927**, 122–123 (2007)
8. N.P. Patel, V. Verma, D. Modi, K.V.R. Murhty, M. Srinivas, Thermoluminescence kinetic features of Eu^{3+} doped strontium pyrophosphate after beta irradiation. RSC Adv. **6**, 77622–77628 (2016)
9. W. Binder, J.R. Cameron, Dosimetric properties of CaF_2: Dy. Health Phys. **17**, 613–618 (1969)
10. P.J. Fox, R.A. Akber, J.R. Prescott, Spectral characteristics of six phosphors used in thermoluminescence dosimetry. J. Phys. D Appl. Phys. **21**, 189–193 (1988)
11. A. Duragkar, A. Muley, N.R. Pawar, V. Chopra, N.S. Dhoble, O.P. Chimankar, S.J. Dhoble, Versatility of thermoluminescence materials and radiation dosimetry—a review. Luminescence **34**, 656–665 (2019)
12. J. Azorín, C. Furetta, A. Scacco, Preparation and properties of thermoluminescent materials. Phys. Stat. Solidi **138**, 9–46 (1993)
13. J. Zeler, J. Cybińska, E. Zych, A new photoluminescent feature in LuPO4: Eu thermoluminescent sintered materials. RSC Adv. **6**, 57920–57928 (2016)
14. M. Kloss, B. Finke, L. Schwarz, D. Haberland, Optical investigation on $Na_3RE(PO_4)_2$ (RE = La, Gd, Eu). J. Lumin. **72**, 684–686 (1997)
15. J. Legendziewicz, M. Guzik, J. Cybinska, VUV spectroscopy of double phosphates doped with rare earth ions. Opt. Mater. **31**, 567–574 (2009)
16. G.B. Nair, S. Tamboli, S.J. Dhoble, H.C. Swart, Comparison of the thermoluminescence properties of $NaCaPO_4$:Dy^{3+} phosphors irradiated by 75 MeV C^{6+} ion and γ-rays. J. Lumin. **224**, 117274–117283 (2020)

17. J.A. Wani, N.S. Dhoble, S.P. Lochab, S.J. Dhoble, Luminescence characteristics of C^{5+} ions and ^{60}Co irradiated $Li_2BaP_2O_7:Dy^{3+}$ phosphor. Nucl. Instrum. Methods Phys. Res. B **349**, 56–63 (2015)
18. H.A. Batal, Absorption spectra of gamma-irradiated sodium phosphate glasses containing vanadium. Nucl. Instrum. Methods Phys. Res. B **124**, 81–90 (1997)
19. C.H. Tsai, J.H.C. Lin, C.P. Ju, Gamma-radiation-induced changes in structure and properties of tetracalcium phosphate and its derived calcium phosphate cement. J. Biomed. Mater. Res. B Appl. Biomater. **80**, 244–252 (2007)
20. S. Fan, C. Yu, D. He, K. Li, L. Hu, Gamma rays induced defect-centers in phosphate glass for radio-photoluminescence dosimeter. Radiat. Meas. **46**, 46–50 (2011)
21. P.P. Mokoena, M.L. Chithambo, V. Kumar, H.C. Swart, O.M. Ntwaeaborwa, Thermoluminescence of calcium phosphate co-doped with gadolinium and praseodymium. Radiat. Meas. **77**, 26–33 (2015)
22. H. Tanaka, Y. Fujimoto, M. Koshimizu, T. Yanagida, T. Yahaba, K. Saeki, K. Asai, Radiophotoluminescence properties of Ag-doped phosphate glasses. Radiat. Meas. **94**, 73–77 (2016)
23. S. Kodaira, T. Kusumoto, H. Kitamura, Y. Yanagida, Y. Koguchi, Characteristics of fluorescent nuclear track detection with Ag^+-activated phosphate glass. Radiat. Meas. **132**, 106252–106260 (2020)
24. P. Godlewska, A. Matraszek, L. Macalik, K. Hermanowicz, M. Ptak, P.E. Tomaszewski, J. Hanuza, I. Szczygieł, Spectroscopic and structural properties of $Na_3RE(PO_4)_2$:Yb. J. Alloy. Comp. **628**, 199–207 (2015)
25. K. Hareesh, R.P. Joshi, S.S. Dahiwale, V.N. Bhoraskar, S.D. Dhole, Synthesis of Ag-reduced graphene oxide nanocomposite by gamma radiation assisted method and its photocatalytic activity. Vacuum **124**, 40–45 (2016)
26. A. Matraszek, I. Szczygieł, B. Szczygieł, Hydrothermal synthesis and characterization of $Na_3Y(PO_4)_2$ phosphate. J. Alloy. Compd. **612**, 411–417 (2014)
27. K. Munirathnam, P.C. Nagajyothi, D. Prakashbabu, B.D.P. Raju, J. Shim, X-ray photoelectron spectroscopy and optical analysis of pure white light emitting Dy^{3+} and Mn^{2+}codoped $Na_3Y(PO_4)_2$ phosphors for solid-state lighting. Ceram. Int. **45**(1), 686–694 (2019)
28. J. Chékir-mzali, K. Horchani-naifer, M. Férid, Synthesis of Er^{3+} -doped $Na_3La(PO_4)_2$ micro-powders and photoluminescence properties. Super Lattice Microstruct. **85**, 445–453 (2015)
29. S. Chemingui, M. Ferhi, K. HorchaniNaifer, M. Férid, Synthesis and luminescence characteristics of Dy^{3+} doped $KLa(PO_3)_4$. J. Lumin. **166**, 82–87 (2015)
30. G.B. Nair, S.J. Dhoble, Highly enterprising calcium zirconium phosphate $CaZr_4(PO_4)_6:Dy^{3+}$, C^{e3}+ phosphor for white light emission. RSC Adv. **5**, 49235–49247 (2015)
31. P.P. Kulkarni, K.H. Gavhane, M.S. Bhadane, V.N. Bhoraskar, S.S. Dahiwale, S.D. Dhole, Investigation of the photoluminescence and novel thermoluminescence dosimetric properties of NaGdF4:Tb3+ phosphors. Mater. Adv. **1**, 1113–1124 (2020)
32. R. Chen, On the calculation of activation energies and frequency factors from glow curves. J. Appl. Phys. **40**, 570–585 (1969)
33. R. Chen, Glow curves with general order kinetics. J. Electrochem. Soc. **116**, 1254–1257 (1969)
34. L.I. Lushihik, Sov. Phys. JETP **3**, 390 (1956)
35. A. Halperin, A.A. Braner, Phys. Rev. **117**, 408 (1960)
36. M.S. Bhadane, K.H. Gavhane, P.P. Kulkarni, S.S. Dahiwale, V.N. Bhoraskar, M.A. More, P.S. Patil, S.D. Dhole, Particle size dependent TL response of CaF2: Dy phosphor for gamma dosimetry. J. Lumin. **223**, 117168–117174 (2020)
37. D.L. Luo, K.N. Yu, C.X. Zhang, G.Z. Li, Thermoluminescence characteristics of MgSO4: Dy, Mn and MgSO4:Dy,P, Cu phosphors. J. Phys. D Appl. Phys. **32**, 3068–3074 (1999)
38. Z.S. Khan, N.B. Ingale, S.K. Omanwar, Thermoluminescence Studies of $CaSO_4$: Dy, P, phosphor. JAAST Mater. Sci. **1**, 277–279 (2014)